IJIE

UTHM Penerbit

INTERNATIONAL JOURNAL OF INTEGRATED ENGINEERING
ISSN: 2229-838X e-ISSN: 2600-7916

Vol. 18 No. 4 (2026) 169-181
https://publisher.uthm.edu.my/ojs/index.php/ijie

Predictive Modelling of Stress and Tensile Properties of Oral Dispersible Film Using Artificial Neural Network

Fetriya Fatihah Nasar[1], Jamaluddin Mahmud[2]*, Noor Fitrah Abu Bakar[1], Nur Asyikin Ahmad Nazri[3]

[1] *Faculty of Chemical Engineering,*
Universiti Teknologi MARA (UiTM), 40450 Shah Alam, MALAYSIA
[2] *Faculty of Mechanical Engineering,*
Universiti Teknologi MARA (UiTM), 40450 Shah Alam, MALAYSIA
[3] *Centre of Foundation Studies,*
Universiti Teknologi MARA (UiTM), Kampus Dengkil, 43800 Dengkil, MALAYSIA

*Corresponding Author: jm@uitm.my
DOI: https://doi.org/10.30880/ijie.2026.18.04.012

Article Info

Received: 30 October 2025
Accepted: 13 May 2026
Available online: 17 June 2026

Keywords

Oral Dispersible Film (ODF), electrospinning, ascorbic acid, tensile, Artificial Neural Network (ANN), Young's modulus

Abstract

An Oral Dispersible Film (ODF) remains a polymeric device designed for easier drug administration in the treatment course, especially for paediatric and geriatric therapy patients, for whom adherence remains a challenge owing to swallowing difficulties. The study employs an Artificial Neural Network (ANN) to assess the tensile properties, specifically the stress and Young's modulus, of PVA electrospun ODFs with κ-carrageenan and ascorbic acid. The ODFs were characterised and their mechanical properties assessed using a tensile mechanical testing apparatus. The ANN model was created using a feed-forward backpropagation neural network. The network was trained with the Levenberg–Marquardt algorithm. The dataset was divided into the training set, validation set, and testing set. These findings provided indications of the ANN's predictive power, demonstrated by R2 = 0.999 with very low mean square error. The highest mean square error was 4.737% for stress and 2.081% for Young's modulus, meaning the model is very accurate. This research shows that modelling based on ANN is time-effective for predicting ODFs' mechanical properties. It optimizes invaluable data elements to formulate process designs related to the prediction and mechanical property relationship to ODFs in the pharmaceutical industry.

1. Introduction

The unique properties of Oral Dispersible Films (ODFs) have attracted interest in the pharmaceutical and nutraceutical markets. ODFs dissolve in the oral cavity instantly and can be taken without water, making them ideal for the easy administration of drugs to children and the elderly [1], [2], [3]. As illustrated in Table 1, they offer a contemporary approach to delivering medications for treating allergies, pain, and neurological conditions [2], and they are included in nutraceuticals and functional foods containing vitamins and antioxidants [1], [3]. ODFs typically consist of hydrophilic, saliva-activated, and rapidly disintegrating polymer matrices, thus improving patient compliance and increasing the availability of the drug for absorption [4], [5], [6].

The mechanical integrity of ODFs, particularly tensile strength, flexibility, and Young's modulus, is essential for the stability of the film during production, handling, packaging, and patient administration [7], [8], [9]. The composition of the polymer will significantly influence the tensile strength, flexibility, and Young's modulus of the ODFs. Polyvinyl alcohol (PVA) is often used because of its solubility in water, biocompatibility, and strength [10], while κ-carrageenan (κ-car) assists in film formation and structural stability. Ascorbic acid (AA) is a thermally sensitive and hydrophilic active pharmaceutical ingredient (API) that has medicinal properties and works as a functional additive with antioxidant activity [1], [11].

Electrospinning is a flexible and cost-effective way to make nanofibrous ODFs with better mechanical and dissolving properties than other methods. Unlike solvent casting and hot-melt extrusion, electrospinning provides superior control over fibre morphology, allows for processing at lower temperatures, and is compatible with heat-sensitive active pharmaceutical ingredients. This is why it is a widely accepted technique for enhancing orally dispersible film systems [12], [13], [14], [15]. However, the prediction of the impact of formulation and processing parameters on the electrospun film tensile properties remains complicated due to the non-linear and complex interplay between composition and mechanical properties of the film.

In this context, Artificial Neural Networks (ANNs) provide a feasible data-driven way for modelling and predicting properties of the materials. Due to their mimicry of the brain's nonlinear pattern recognition capabilities, ANNs have become very useful for revealing hidden relationships between input variables of the experiments and the mechanical output variables [16], [17], [18]. The Levenberg-Marquardt (LM) technique, which is commonly implemented in the discipline of engineering and material modelling, is noted for its rapid convergence and favourable output predictions for moderately sized datasets [19]. Previous studies have demonstrated the efficacy of ANNs in predicting tensile strength for various materials such as nano-TiO_2-coated cotton [20], fibre-reinforced composites [21], and polymer films produced through fused deposition modelling [22]. However, predictive formulation studies in ODF systems remain [6], [23], indicating a considerable research gap in predictive formulation studies.

This research focuses on constructing an ANN-based predictive model for estimating tensile stress and Young's modulus for electrospun natural ODF formulations made of PVA κ-car and AA, while building a predictive model based on a feed-forward backpropagation network trained using the Levenberg-Marquardt. This model correlates the tensile results with the experimental data consisting of strain, force, and displacement. This study shows the applicability of ANN modelling as a practically useful predictive tool for determining the mechanical characteristics of ODFs, thus reducing experimental efforts and facilitating the rapid data-driven optimisation of formulations for the pharmaceutical nanofiber development, whereby experimental and computational methodologies are employed in unison.

2. Materials and Methods

2.1 Solution Preparation of PVA/κ-Car/AA ODF

A solution of PVA was prepared by dissolving 2.4g of PVA in 20mL of deionised (DI) water. The mixture was heated using a water bath at 90°C with constant stirring at 360 rpm for 2 hours (kept closed). Meanwhile, κ-carrageenan (κ-car) solution was prepared by dissolving 1g of κ-car powder in 100mL of DI water with rapid stirring in a water bath at 80°C for 30 minutes. The κ-car solution was being sonicated at 60% amplitude for 3 minutes to remove air bubbles that were entrapped, followed by another heating for 1 hour at 80°C. Afterwards, PVA and κ-car solutions were mixed up in a 90:10 (v/v) ratio, which is 16mL and 4mL of PVA and κ-car, respectively. The blended solution was heated until it was completely dissolved under a constant stirring of 360 rpm. The solution was then cooled down to room temperature. AA was dispersed into the mixture at different concentrations (0.2, 0.6, 1.0, 1.4, 1.8, and 2.2g of AA) and stirred until the solution was homogeneous.

2.2 Electrospinning

Prepared solution of PVA/κ-car/AA was drawn into a 5mL syringe with a 23G needle attached at the tip of the syringe. The setup for this experiment (Fig. 1) involved connecting the injector to a 16kV power supply, and the flow rate was set to 0.4 mL/hr. The distance between the collector plate and the tip of the needle was 14 to 16 cm (Table 1). Aluminium foil was used to wrap the collector plate that will be collecting the ODF nanofibers. Ambient temperature was kept throughout the electrospinning process.

2.3 Tensile Test

Tensile tests were carried out using a Universal Testing Machine (UTM, Tinius Olsen H50KT) on the ODF specimens to characterise their mechanical behaviour. ODF's film was cut (15mm x 70mm) and fixed onto the probe of the tensile machine grip. The film was clamped with a recording of the point at which the film was broken. This test was performed at a speed of 5mm/min and was repeated for six other films with different concentrations (1, 3, 5, 7, 9, and 11 w/v%). For each concentration, three specimens were tested. For a standard tensile test, the load-displacement curves were generated, whereby the strain and stress values were calculated using Eq. (1) and Eq. (2). The ANN model was trained using experimental data obtained from tensile testing. Load and displacement measurements were used to calculate stress and Young's Modulus based on Eq. (1-3). These computed values, together with the formulation parameters, were used as input-output datasets for training the ANN.

2.3.1 Measuring Tensile Properties (Young's Modulus, E)

The standard outputs from a Tensile Test are the Load-Elongation graphs, where the machine converts these values into a Stress-Strain curve. Based on the mechanics of materials, the Stress-strain curves define the tensile behaviour of a material, where the material stiffness, namely Young's Modulus, E, was determined using Eq. (3).

Table 1 *Parameters used in electrospinning*

Electrospinning parameters	Value
Flow rate (ml/hr)	0.4 - 0.6
Voltage (kV)	15 - 16
Distance from tip to collector plate (cm)	14 to 16
Needle	23G

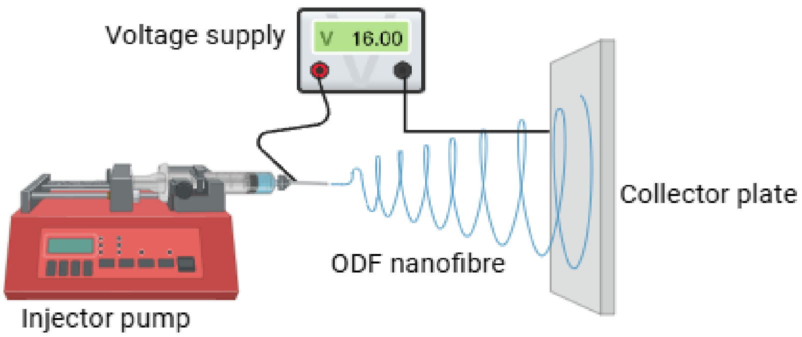

Fig. 1 *Electrospinning setup*

$$\varepsilon = \frac{\Delta L}{L} \quad (1)$$

$\varepsilon = strain$ (m/m)
$\Delta L = displacement$ (m)
$L = length\ (m)$

$$\sigma = \frac{F}{A} \quad (2)$$

$\sigma = stress\ (m/m)$
$F = load$ (N)
$A = cross\text{-}sectional\ area$ (mm^2)

$$\sigma = E\ \varepsilon \quad (3)$$

$\sigma = stress\ (MPa)$
$E = young\ modulus$
$\varepsilon = strain$

2.4 Prediction of Stress and Young's Modulus of ODFs for Different Concentrations Using Artificial Neural Network (ANN)

An Artificial Neural Network is an attempt to imitate the way human brains process information [18]. Fig. 2 shows a schematic diagram of how the ANN models work using a hidden neuron. ANN models used in this study were implemented using MATLAB R2018b, where a three-layer model was trained, and predictions were made using the neural fitting tool (*nftool*). The prediction utilises a feed-forward backpropagation neural network trained using the Levenberg–Marquardt algorithm. This is accessed through the *trainlm* function [24], [25]. 60 datasets generated from the tensile tests were used and randomly divided into three parts (testing, validation, and training). This data has two inputs and one output for both prediction (stress and young modulus).

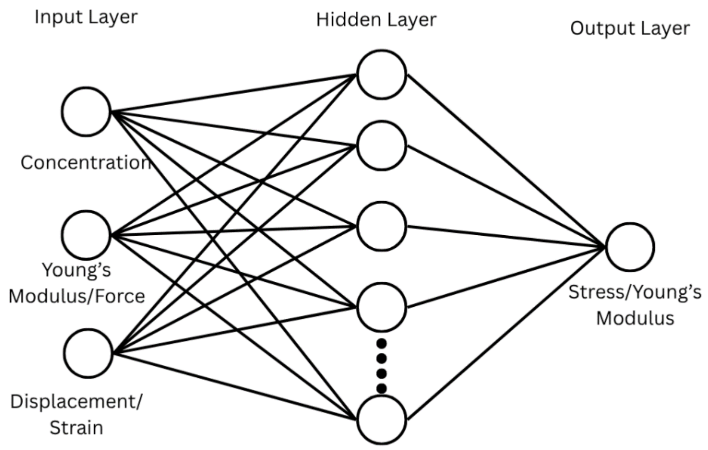

Fig. 2 *Schematic diagram of an ANN*

Tables 2 and 3 summarize the configurations of the ANN models developed to predict stress (MPa) and Young's modulus (MPa), respectively. For stress prediction, the input variables are load (m/m), displacement (MPa), and concentration (w/v%), while for Young's modulus prediction, the inputs include stress (MPa), strain (m/m), and concentration (w/v%). In both models, the output corresponds to the target mechanical property (stress or Young's modulus). Each ANN employs a single hidden layer with 10 neurons and is trained using the Levenberg–Marquardt algorithm. The dataset is consistently divided into 90% training, 5% validation, and 5% testing to ensure reliable model performance and generalization. Then, the count of hidden layer neurons for each input dataset was adjusted from 1 to 10 systematically (Fig. 3), and the number with the optimal results was selected [18].

Figure 3 illustrates the architecture of the function-fitting artificial neural network (ANN) employed in this study. The network consists of an input layer, a single hidden layer, and an output layer. The input layer receives the experimental variables, which are fed into the hidden layer comprising 10 neurons. Each neuron processes the inputs through weighted connections and biases, followed by a nonlinear activation function to capture complex relationships within the data. The processed signals are then passed to the output layer, which produces a single output value corresponding to the predicted target parameter (either stress or Young's modulus). The structure represents a typical feedforward neural network designed for function approximation, where the mapping between input variables and output is learned during training.

This architecture enables the model to effectively capture nonlinear dependencies between the input parameters and the mechanical properties being predicted. The Levenberg-Marquardt algorithm was used as it typically requires more memory but less time. Training automatically stops when generalisation stops improving, as indicated by an increase in the mean square error of the validation samples, and also iterative algorithms like *trainlm* consistently decrease the performance function with every iteration [24]. The dataset for both predictions was divided into 90% for training, 5% for validation, and 5% for testing. Training was done multiple times to achieve a small MSE value. MSE value is important to ensure the model is not overfitting. The Mean Squared Error (MSE) is a regularly used loss function in (ANN) to quantify the accuracy of a prediction model. The predicted value of the ANN was compared with the experimental value, and the error was calculated. Lower MSE (Eq. 4) implies higher model accuracy, since it means the predicted values are closer to the actual values.

$$MSE = \frac{1}{n}\sum_{i=1}^{n}\left(Y_i - \hat{Y}_i\right)^2 \tag{4}$$

3. Results and Discussion

3.1 Predicted Stress, σ, Values Using ANN

The training was done multiple times to achieve a lower MSE value. Mean Squared Error (MSE) is the average squared difference between outputs and targets. The results are shown in Table 4. Lower values are better, and zero means no error. The regression value is also important to get the best-fit line model. Regression value (R) measures the correlation between outputs and targets. An R value of 1 means a close relationship. The regression value (R) shows a nearly perfect fit between the experimental and predicted values, which indicates a best-fit model. R value is 0.999 for validation, training, and testing, which also shows a small MSE value. Fig. 4 and Fig. 5 show the regression plot and performance plot for this ANN model prediction. The regression plots in Fig. 4 show the training, validation, and testing performance of the ANN model trained with the Levenberg–Marquardt (LM) algorithm. All datasets achieved regression coefficients (R^2) of 0.99999, indicating excellent model accuracy.

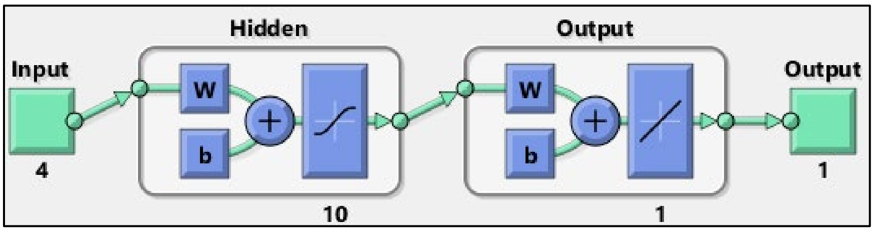

Fig. 3 *Function fitting neural network*

Table 2 *Parameters used in the ANN model for predicting stress (MPa)*

Parameter	
Input	Load (m/m), Displacement (MPa), Concentration (w/V %)
Output	Stress (MPa)
Hidden layer	10
Algorithm	Levenberg-Marquardt
Training/validation/testing	90%/5%/5%

Table 3 *Parameters used in the ANN model for predicting Young's modulus (MPa)*

Parameter	
Input	Stress (MPa) Strain (m/m) Concentration (w/V %)
Output	Young's modulus, *E* (MPa)
Hidden layer	10
Algorithm	Levenberg-Marquardt
Training/validation/testing	90%/5%/5%

Table 4 *Train network results*

	MSE	R^2
Training	3.22329×10^{-11}	0.99999
Validation	1.90330×10^{-11}	0.99999
Testing	4.00142×10^{-11}	0.99999

Fig. 5 regression analysis illustrates how all predicted and actual values correlate with each other and with each dataset during training, validating, and testing. The regression graphs show perfect linear relationships, and the model produces R values of 0.9999, confirming outstanding performance. In the training dataset, the predicted and actual results demonstrated strong correlation and effective learning, and the model validation and testing results demonstrated effective model performance on all data sets. The overall regression graph shows the model has the capacity to generate accurate results for the entire dataset. The overall regression graph shows the model has the capacity to generate accurate results for the entire dataset. The regression results in the performance curve show that the model displayed minimal difference during the whole process of training and evaluation, which aligns with the rest of the results. The regression results in the performance curve show that the model displayed minimal difference during the whole process of training and evaluation, which aligns with the rest of the results. The regression analyses provide better predictive performance, indicating that the neural network produces reliable output as a modelling tool. The regression results for the predictions of film materials based on artificial neural networks show strong linearity and high precision, where R values are often greater than 0.98 in most studies. For instance, Amor et al. demonstrated the capability of ANN to predict the tensile strength of nano titanium dioxide-coated cotton film and achieved R values of almost 0.99 for training and 1.00 for testing, with the regression plot corroborating the strong prediction-experimental tensile value correlation. Likewise, Ali et al. [22] demonstrate in their regression analysis on polymer films fabricated by FDM that the tensile strengths predicted by ANN are closely aligned with the experimental values, attaining a maximum error margin of 8.91% and vastly superior to the correlation and predictive prowess of conventional regression models.

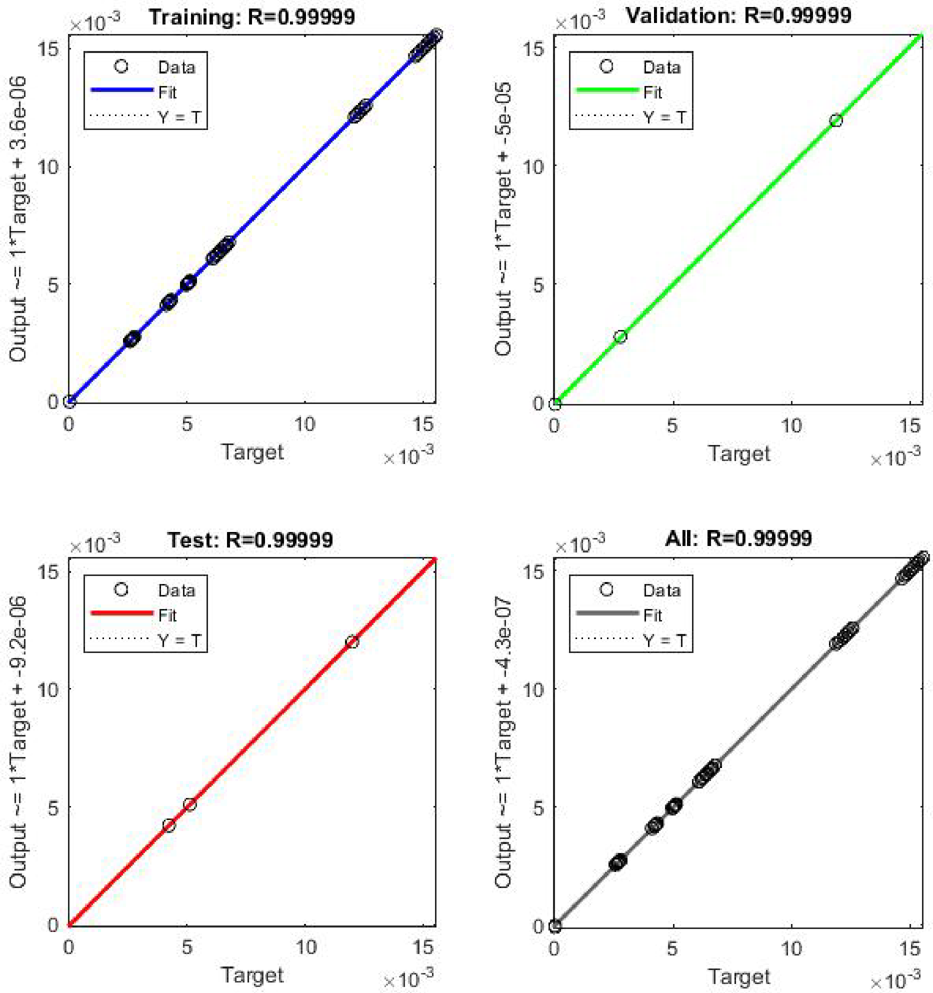

Fig. 4 *Regression graphs of the ANN model performance depict the outcomes for (a) Training; (b) Validation; (c) Testing; and (d) All datasets, with coefficients (R) approaching 1 for stress prediction*

As indicated in Fig. 6, the performance plot achieved a minimum Mean Squared Error (MSE) of 1.9033×10^{-9} at epoch 14, which illustrates convergence with minimal overfitting. The remaining deviation between predicted and experimental tensile stress values confirms that the LM algorithm was able to model the nonlinear mechanical behaviour of the polymeric ODF matrix. The network also demonstrates a significant reduction in error during the initial phase of training as a result of the sharpening of weights for better predictions. The training, validation, and testing curves showed a uniformly converging trend, which indicates the model does not overfit or underfit, yet performs exceptionally well on novel data. The training approach achieved optimal performance as the model showed no signs of instability during the stable convergence phase. The combined effect of the test, validation, and training curves showed a consistent drop, which indicates the network can successfully be deployed in practice. The model reached its lowest error values, which prove it has the exact connection between input and output data. The performance curve demonstrates that the model achieved successful convergence while maintaining both experimental and predictive accuracy. Similar high-accuracy predictions were reported by Üstün et al. [19] and Amor et al. [20]. These findings validate that the developed ANN model provides a reliable computational tool for estimating tensile stress behaviour in electrospun ODFs, minimising the need for extensive experimental testing.

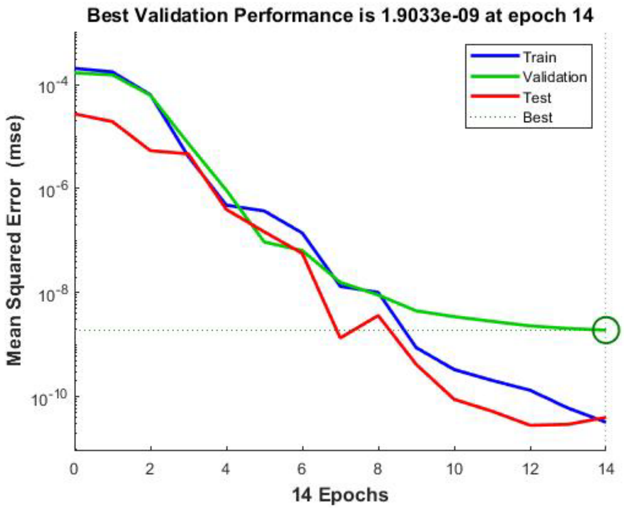

Fig. 5 *The training performance graph of the ANN model illustrates the decrease of mean squared error (MSE) throughout epochs, with optimal validation performance of 1.9033 × 10^{-9} attained at epoch 14*

3.2 Predicted Tensile Properties (Young's Modulus, E) Using ANN

The parameters used are being compared with the experimental value (Table 5). The training was done multiple times to achieve a lower MSE value. MSE is the average squared difference between outputs and targets. The results are shown in Table 4. Lower values are better, and zero means no error. The regression value is also important to get the best-fit line model. Regression value (R) measures the correlation between outputs and targets. An R value of 1 means a close relationship. The regression value (R) shows a nearly perfect fit between the experimental and predicted values, which indicates a best-fit model. R value is 0.999 for validation, training, and testing, which also shows a small MSE value. Fig. 6 and Fig. 7 show the regression plot and performance plot for this ANN model prediction. Fig. 6 illustrates the regression plots for the prediction of Young's modulus during training, validation, and testing phases. The R^2 value of 0.99999 across all datasets indicates that the ANN model achieved exceptional accuracy and generalisation.

Table 5 *Train network results*

	MSE	R^2
Training	3.23738×10^{-10}	0.99999
Validation	2.97387×10^{-9}	0.99999
Testing	9.64720×10^{-11}	0.99999

Regression plots (Fig. 6) display predicted values of Young's modulus within training, validation, and testing datasets. These values are strongly correlated, and a regression correlation of 0.9999 indicates that most of the data cluster around the line. Such close agreement indicates that the ANN predicted the value with minimal systematic error. ANN predictions of Young's modulus for the ODF film demonstrate an almost perfect correlation with experimental values, as indicated by the regression R values close to 0.9999 during training, validation, and testing. Other studies employing artificial neural networks with film-type materials, such as metallic glasses and metal alloy films, tend to report similarly strong, though somewhat diminished, regression precision. For instance, Han et al. [26] obtained R values between 0.97 and 0.99 when they modelled Young's modulus of thin film material, whereas Galimzyanov et al. [27] indicated a comparably high but imperfect ANN correlation, which implies moderate but significant differences between their prediction outputs and experimental results. The ODF result almost perfect regression fit, creates a new standard for how one can predict the mechanical properties of film materials.

The best validation performance was achieved at epoch 8, when the MSE was 2.9739×10^{-9} (Fig. 7). The ANN continued to produce reliable predictions even though it was slightly overfitting. A low MSE value means that this model might be able to make accurate predictions, which shows this model is strongly compatible with both training and testing data. The ANN's high accuracy in determining Young's modulus shows that it can comprehend how PVA/κ-car/AA-based films appear when they are stretched. Young's modulus is related to the flexibility and mechanical reliability of ODF. Precise modelling improves the handling of films and the stability of drugs [7], [8], [9]. The results obtained in this work correspond with the findings of Rehman et al. [21] and Ali et al. [22], confirming the efficacy of ANN applications in predicting the mechanical properties of polymers. This shows that minor overfitting is present, but no significant bias. As shown in the performance plot graph (Fig. 7), the ANN model clearly displays a steady and quick decline in mean squared error over epochs, with validation and training errors tightly connected and minimal overfitting, demonstrating robust optimisation and generalisation. In comparison, Gao et al. [28] presented an epoch graph from an ANN model for nanolaminate film simulation, where the minimum validation MSE (0.0294) was reached relatively early (at epoch 8), but both training and validation errors plateaued at higher values than the Fig. 7 results, indicating less effective model tuning for those film samples. These comparisons illustrate how the ANN model for ODF film prediction achieves both lower final error and more optimum training dynamics than several previously published ANN research targeting film materials.

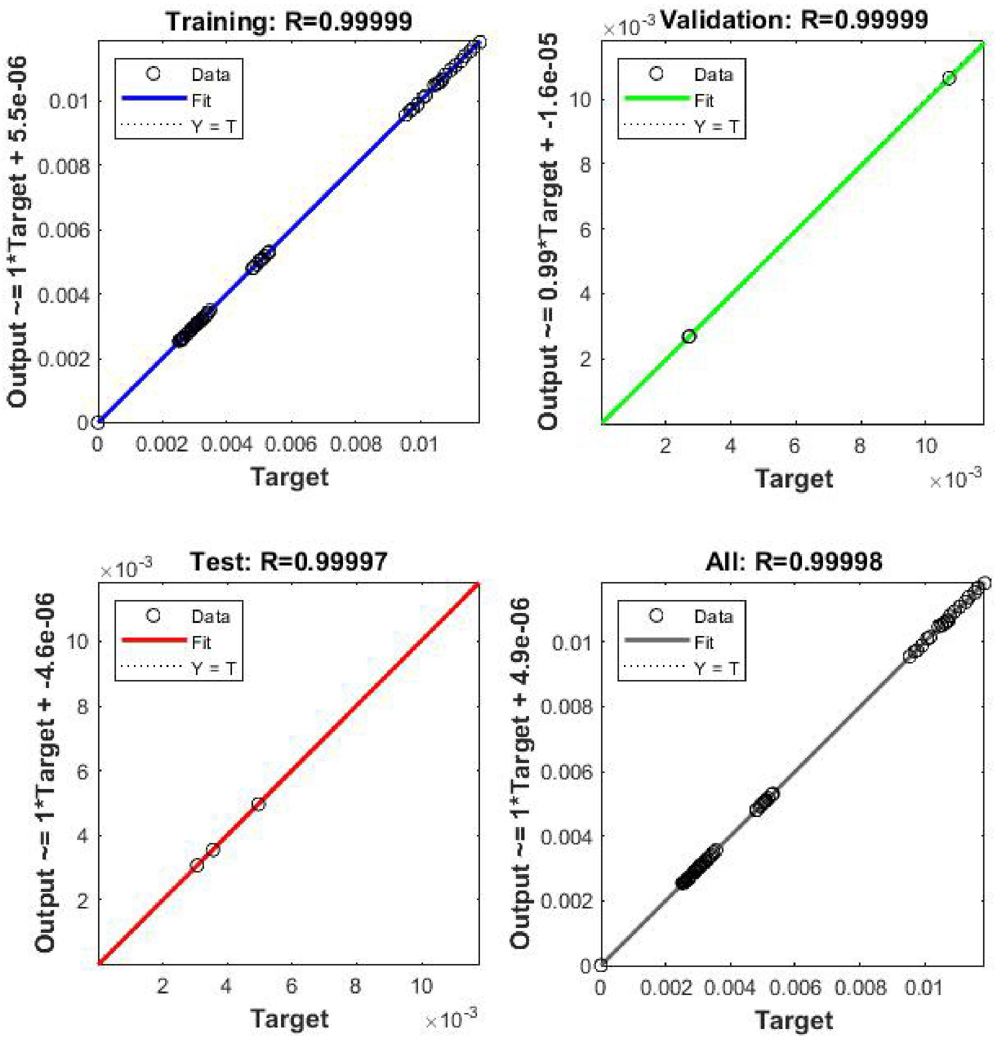

Fig. 6 *Regression graphs of the ANN model performance depict the outcomes for (a) Training; (b) Validation; (c) testing; and (d) All datasets, with coefficients (R) approaching 1 for Young's modulus prediction*

3.2.1 Comparison of Experimental and Prediction Values Using ANN

Table 6 below shows the percentage deviation between ANN-predicted and experimental data, which was evaluated to validate model reliability. The highest deviations reported were 1.62% for tensile stress and 4.70%

for Young's modulus, but the smallest deviation approached 0% in both cases. These findings validate the ability of the ANN model. The minor discrepancy suggests the LM algorithm has successfully optimized the convergence of weights, avoiding overfitting while maintaining reliable predictions. Earlier studies of mechanical modelling based on artificial neural networks [19], [21], [29] have reported similar performance metrics. This highlights the importance of artificial neural network modelling for predictive optimization in the electrospun ODF fabrication.

Table 6 *Error percentage between experimental and ANN value for Young's modulus, E*

Input			Stress, σ		Young Modulus, E		Percentage error (%)	
Concentration, w/v%	Strain, %	Load, N	Experimental data, MPa	ANN model, MPa	Experimental data, MPa	ANN model, MPa	σ	E
1	1.71	1.02	0.00608	0.00609	0.0036	0.0036	0.13	0.04
1	1.76	1.03	0.00611	0.00611	0.0035	0.0035	0.02	0.62
1	1.82	1.05	0.00622	0.00622	0.0034	0.0034	0.05	0.16
1	1.87	1.06	0.00628	0.00628	0.0034	0.0034	0.05	0.02
1	1.93	1.08	0.00639	0.00639	0.0033	0.0033	0.02	0.54
1	1.99	1.09	0.00644	0.00645	0.0032	0.0032	0.14	0.30
1	2.04	1.11	0.00656	0.00657	0.0032	0.0032	0.11	0.74
1	2.1	1.12	0.00662	0.00661	0.0032	0.0032	0.11	0.04
1	2.16	1.12	0.00667	0.00667	0.0031	0.0031	0.04	0.84
1	2.21	1.14	0.00678	0.00678	0.0031	0.0031	0.06	0.07
3	1.49	0.693	0.00411	0.00411	0.0028	0.0028	0.05	0.09
3	1.51	0.693	0.00411	0.00412	0.0027	0.0027	0.15	0.41
3	1.54	0.709	0.00421	0.00421	0.0027	0.0027	0.12	1.33
3	1.56	0.712	0.00422	0.00422	0.0027	0.0027	0.07	1.13
3	1.58	0.712	0.00422	0.00422	0.0027	0.0027	0.02	0.67
3	1.61	0.712	0.00422	0.00423	0.0026	0.0026	0.14	0.11
3	1.64	0.72	0.00427	0.00427	0.0026	0.0026	0.09	0.18
3	1.67	0.731	0.00433	0.00433	0.0026	0.0026	0.02	0.61
3	1.7	0.731	0.00433	0.00426	0.0025	0.0026	1.62	0.35
3	1.72	0.731	0.00433	0.00433	0.0025	0.0025	0.00	1.04
5	1.11	2.01	0.0119	0.0119	0.011	0.011	0.17	0.75
5	1.13	2.03	0.0120	0.0120	0.011	0.011	0.08	0.37
5	1.15	2.04	0.0121	0.0121	0.011	0.011	0.17	0.08
5	1.17	2.06	0.0122	0.0122	0.010	0.010	0.08	0.01
5	1.2	2.06	0.0122	0.0122	0.010	0.010	0.25	0.16
5	1.22	2.07	0.0123	0.0123	0.010	0.010	0.08	0.18
5	1.24	2.08	0.0123	0.0123	0.010	0.010	0.16	0.40
5	1.27	2.09	0.0124	0.0124	0.010	0.010	0.32	0.26
5	1.29	2.11	0.0125	0.0125	0.010	0.010	0.08	0.08
5	1.32	2.12	0.0126	0.0125	0.010	0.010	0.48	0.08
7	0.828	0.431	0.00256	0.00257	0.0031	0.0031	0.55	0.27
7	0.844	0.437	0.00259	0.00260	0.0031	0.0031	0.23	0.37
7	0.861	0.447	0.00265	0.00265	0.0031	0.0031	0.19	0.06
7	0.875	0.45	0.00267	0.00266	0.0031	0.0031	0.22	0.01
7	0.887	0.45	0.00267	0.00267	0.0030	0.0030	0.07	0.23
7	0.903	0.45	0.00267	0.00267	0.0030	0.0030	0.11	0.48
7	0.92	0.45	0.00267	0.00268	0.0029	0.0029	0.34	0.72
7	0.935	0.456	0.00270	0.00271	0.0029	0.0029	0.26	0.46
7	0.948	0.465	0.00276	0.00276	0.0029	0.0029	0.11	0.15
7	0.961	0.468	0.00278	0.00278	0.0029	0.0029	0.07	0.27

Input			Stress, σ		Young Modulus, E		Percentage error (%)	
Concentration, w/v%	Strain, %	Load, N	Experimental data, MPa	ANN model, MPa	Experimental data, MPa	ANN model, MPa	σ	E
9	0.934	0.836	0.00496	0.00496	0.0053	0.0053	0.04	0.07
9	0.949	0.843	0.00500	0.00500	0.0053	0.0053	0.06	0.16
9	0.967	0.843	0.00500	0.00500	0.0052	0.0052	0.04	0.07
9	0.984	0.846	0.00502	0.00502	0.0051	0.0051	0.06	0.09
9	1	0.855	0.00507	0.00507	0.0051	0.0051	0.02	0.22
9	1.02	0.862	0.00511	0.00511	0.0050	0.0050	0.02	0.38
9	1.03	0.862	0.00511	0.00511	0.0050	0.0050	0.02	0.26
9	1.04	0.862	0.00511	0.00511	0.0049	0.0049	0.02	0.15
9	1.06	0.862	0.00511	0.00511	0.0048	0.0048	0.02	0.06
9	1.07	0.865	0.00513	0.00513	0.0048	0.0048	0.04	0.05
11	1.24	2.47	0.0147	0.0147	0.012	0.012	0.07	0.29
11	1.27	2.49	0.0148	0.0148	0.012	0.012	0.07	0.14
11	1.29	2.51	0.0149	0.0149	0.012	0.012	0.13	0.18
11	1.32	2.52	0.0150	0.0150	0.011	0.011	0.07	0.23
11	1.34	2.54	0.0151	0.0151	0.011	0.011	0.13	0.25
11	1.37	2.56	0.0152	0.0152	0.011	0.011	0.07	0.04
11	1.4	2.58	0.0153	0.0153	0.011	0.011	0.07	4.70
11	1.43	2.59	0.0154	0.0154	0.011	0.011	0.19	0.38
11	1.45	2.61	0.0155	0.0155	0.011	0.011	0.06	0.28
11	1.48	2.63	0.0156	0.0156	0.011	0.011	0.06	0.20

4. Conclusion

This study successfully demonstrated the fabrication of electrospun ODFs composed of PVA/κ-car/AA, achieving mechanical properties suitable for pharmaceutical applications. The tensile stress and Young's modulus that correlate to ODFs were accurately predicted with the use of the LM algorithm and ANN model. The model achieved an R^2 of around 0.9999 and extremely low MSE values. The MSE values for both parameters are as follows:

i. For stress prediction ANN, the MSE values were 3.22329×10^{-11} for training, 1.90330×10^{-11} for validation, and 4.00142×10^{-11} for testing.
ii. For Young's modulus prediction ANN, the MSE values were 3.23738×10^{-10} for training, while 2.97387×10^{-9} and 9.64720×10^{-11} were for validation and testing, respectively.

This level of predictiveness lessens the need for various experimental attempts, which aids in the optimization of formulation and various other process parameters. ANN-based modelling continues to indicate its practical use for the advancement of polymeric drug delivery systems. It also highlights the development, quality assurance, and scalability of the system. Improving the ANN framework by pairing it with the mentioned techniques in finite element modelling or deep learning is suggested to tackle future challenges and improve the precision of the model with its utilization in other pharmaceutical systems.

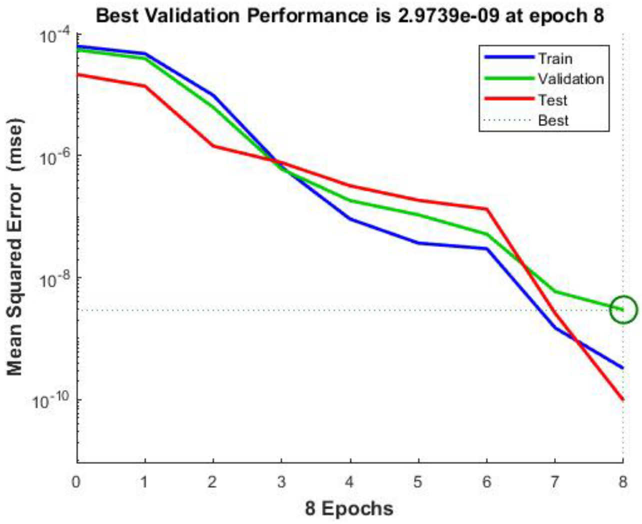

Fig. 7 *Training performance plot for the ANN model, illustrating the decrease in mean squared error (MSE) over epochs*

Acknowledgement

We would like to express our gratitude to the Ministry of Higher Education (MOHE) Malaysia and Universiti Teknologi MARA for sponsoring this research under the Fundamental Research Grant Scheme (Grant no.: FRGS/1/2024/TK10/UITM/03/1).

Conflict of Interest

The authors declare that there is no conflict of interest regarding the publication of the paper.

Author Contribution

*The authors confirm contribution to the paper as follows: **study conception and design**: Fetriya Fatihah Nasar, Jamaluddin Mahmud; **data collection**: Fetriya Fatihah Nasar; **analysis and interpretation of results**: Fetriya Fatihah Nasar, Jamaluddin Mahmud; **draft manuscript preparation**: Fetriya Fatihah Nasar, Jamaluddin Mahmud, Noor Fitrah Abu Bakar, Nur Asyikin Ahmad Nazri. All authors reviewed the results and approved the final version of the manuscript.*

References

[1] S. C. Palezi, S. S. Fernandes, S. C. Barbosa, E. G. Primel, and V. G. Martins, "Orally disintegrating films based on sodium alginate as a carrier vehicle for vitamin C," *Int. J. Food Sci. Technol.*, vol. 59, no. 2, pp. 864–871, 2024, doi: 10.1111/ijfs.16845.

[2] B. S. Rawat *et al.*, "A Review on Orodispersible Film-based Novel Drug Delivery System," *Res. J. Pharm. Technol.*, vol. 17, no. 7, pp. 3480–3488, Jul. 2024, doi: 10.52711/0974-360X.2024.00544.

[3] K. Khatreja and D. Santhiya, "Physicochemical characterization of novel okra mucilage/hyaluronic acid-based oral disintegrating films for functional food applications," *Int. J. Biol. Macromol.*, vol. 278, no. P1, p. 134633, 2024, doi: 10.1016/j.ijbiomac.2024.134633.

[4] M. Reuther, N. Rollet, F. Debeaufort, and O. Chambin, "Orodispersible films prepared by hot-melt extrusion versus solvent casting," *Int. J. Pharm.*, vol. 675, no. March, 2025, doi: 10.1016/j.ijpharm.2025.125536.

[5] M. S. Pacheco, D. Barbieri, C. F. da Silva, and M. A. de Moraes, "A review on orally disintegrating films (ODFs) made from natural polymers such as pullulan, maltodextrin, starch, and others," *Int. J. Biol. Macromol.*, vol. 178, pp. 504–513, 2021, doi: 10.1016/j.ijbiomac.2021.02.180.

[6] E. M. Maher, A. M. A. Ali, H. F. Salem, and A. A. Abdelrahman, "In vitro/in vivo evaluation of an optimized fast dissolving oral film containing olanzapine co-amorphous dispersion with selected carboxylic acids," *Drug Deliv.*, vol. 23, no. 8, pp. 3088–3100, 2016, doi: 10.3109/10717544.2016.1153746.

[7] R. M. Zaki *et al.*, "Fabrication and characterization of orodispersible films loaded with solid dispersion to enhance Rosuvastatin calcium bioavailability," *Saudi Pharm. J.*, vol. 31, no. 1, pp. 135–146, 2023, doi: 10.1016/j.jsps.2022.11.012.

[8] A. Hussain, S. Latif, N. Abbas, M. Irfan, M. S. Arshad, and N. I. Bukhari, "Hydroxypropyl cellulose-based orally disintegrating films of promethazine HCL for the treatment of motion sickness," *Trop. J. Pharm. Res.*, vol. 17, no. 6, pp. 991–996, 2018, doi: 10.4314/tjpr.v17i6.2.

[9] T. S. Makram *et al.*, "Formulation of Saxagliptin Oral Films: Optimization, Physicochemical Characterization, In-Vivo Assessment, and In-Vitro Real-Time Release Monitoring via a Novel Polyaniline Nanoparticles-Based Solid-Contact Screen Printed Ion-Selective Electrode," *AAPS PharmSciTech*, vol. 25, no. 5, pp. 1–17, Feb. 2024, doi: 10.1208/s12249-024-02828-4.

[10] T. P. A. Tran, A. H. Luong, and W. C. Lin, "Characterizations of Centrifugal Electrospun Polyvinyl Alcohol/Sodium Alginate/Tamanu Oil/Silver Nanoparticles Wound Dressing," *IEEE Trans. Nanobioscience*, vol. 23, no. 2, pp. 368–377, Apr. 2024, doi: 10.1109/TNB.2024.3371224.

[11] S. C. Palezi, S. S. Fernandes, and V. G. Martins, "Oral disintegration films: applications and production methods," Oct. 01, 2023, *Springer*. doi: 10.1007/s13197-022-05589-9.

[12] S. Ardalkar, D. Mathure, A. Pawar, and R. Awasthi, "Formulation and optimization of electrospun nanofiber films for ultrafast delivery of domperidone: In vitro and in-vivo characterization," *J. Drug Deliv. Sci. Technol.*, vol. 95, May 2024, doi: 10.1016/j.jddst.2024.105645.

[13] D. Yu, "Electrospun Biomolecule-Based Drug Delivery Systems," pp. 1–6, 2023.

[14] A. Rohani Shirvan, N. Hemmatinejad, S. H. Bahrami, and A. Bashari, "A comparison between solvent casting and electrospinning methods for the fabrication of neem extract-containing buccal films," *J. Ind. Text.*, vol. 51, no. 1, pp. 311S-335S, 2022, doi: 10.1177/15280837211027785.

[15] S. Lian, D. Lamprou, and M. Zhao, "Electrospinning Technologies for the Delivery of Biopharmaceuticals: Current Status and Future Trends," *Int. J. Pharm.*, p. 123641, Nov. 2023, doi: 10.1016/j.ijpharm.2023.123641.

[16] D. L. Galata *et al.*, "Fast, spectroscopy-based prediction of in vitro dissolution profile of extended release tablets using artificial neural networks," *Pharmaceutics*, vol. 11, no. 8, Aug. 2019, doi: 10.3390/pharmaceutics11080400.

[17] P. Spanu and B. F. Abaza, "Tensile Strength Prediction of Fiberglass Polymer Composites Using Artificial Neural Network Model," *Mater. Plast.*, vol. 59, no. 2, pp. 111–118, 2022, doi: 10.37358/MP.22.2.5590.

[18] P. Singh, P. Dwivedi, and V. Kant, "A hybrid method based on neural network and improved environmental adaptation method using Controlled Gaussian Mutation with real parameter for short-term load forecasting," May 01, 2019, *Elsevier Ltd*. doi: 10.1016/j.energy.2019.02.141.

[19] B. Üstün, H. Aydın, S. N. Koç, A. Uluslu, and Kurtan, "Electrospun polyethylenimine (PEI)-derived nitrogen enriched carbon nanofiber for supercapacitors with artificial neural network modeling," *J. Energy Storage*, vol. 73, Dec. 2023, doi: 10.1016/j.est.2023.108970.

[20] N. Amor, M. T. Noman, A. Ismail, M. Petru, and N. Sebastian, "Use of an Artificial Neural Network for Tensile Strength Prediction of Nano Titanium Dioxide Coated Cotton," *Polymers (Basel).*, vol. 14, no. 5, pp. 1–11, 2022, doi: 10.3390/polym14050937.

[21] F. Rehman, H. Li, S. A. Khokhar, U. J. Malik, A. Hamza, and S. Song, "Development of an artificial neural network (ANN) based model for tailoring the fracture response of eco-friendly engineered geopolymer composites (EGC)," *Next Mater.*, vol. 8, no. February, p. 100812, 2025, doi: 10.1016/j.nxmate.2025.100812.

[22] D. Ali, A. F. Huayier, and A. Enzi, "Parametric Prediction of FDM Process to Improve Tensile Properties Using Taguchi Method and Artificial Neural Network," *Adv. Sci. Technol. Res. J.*, vol. 17, no. 4, pp. 130–138, 2023, doi: 10.12913/22998624/169572.

[23] H. Lou, J. I. Chung, Y. H. Kiang, L. Y. Xiao, and M. J. Hageman, "The application of machine learning algorithms in understanding the effect of core/shell technique on improving powder compactability," *Int. J. Pharm.*, vol. 555, no. September 2018, pp. 368–379, 2019, doi: 10.1016/j.ijpharm.2018.11.039.

[24] F. F. Nasar, N. F. A. Bakar, and J. Mahmud, "Prediction of In-vitro Dissolution Profile for Oral Dispersible Film (ODF) using Artificial Neural Network," *2024 IEEE 22nd Student Conf. Res. Dev. SCOReD 2024*, pp. 192–196, 2024, doi: 10.1109/SCORED64708.2024.10872643.

[25] M. Naufal *et al.*, "Predictive Modelling of Hybrid Composite Laminates Buckling Behaviour using Finite Element Analysis , Refined Response Surface Methodology and Artificial Neural Network Models with Different Data Sizes," vol. 23, no. 1, pp. 179–211, 2026, doi: 10.24191/jmeche.v23i1.9426.

[26] G. Han, K. P. Marimuthu, and H. Lee, "Evaluation of thin film material properties using a deep nanoindentation and ANN," 2022. doi: 10.1016/j.matdes.2022.111000.

[27] A. V. Galimzyanov, Bulat N., Maria A. Doronina Mokshin, "Machine learning-based prediction of elastic properties of.pdf."

[28] M. Gao, J. Meng, N. Ma, M. Li, and L. Liu, "Artificial neural network–based constitutive relation modelling for the laminated fabric used in stratospheric airship," *Compos. Adv. Mater.*, vol. 31, 2022, doi: 10.1177/26349833211073146.

[29] M. H. Hidzer, N. H. Sapiee, W. M. N. W. A. Rahman, C. H. Le, H. Q. Nguyen, and J. Mahmud, "Leucaena-Silicone Biocomposite: Experimentation, Quantification and Prediction of Mechanical Properties for Potential Applications in Medicine and Healthcare," *Int. J. Automot. Mech. Eng.*, vol. 22, no. 2, pp. 12332–12343, 2025, doi: 10.15282/ijame.22.2.2025.7.0944.